

A Multiband Compact Low-Profile Planar Antenna Based on Multiple Resonant Stubs

Jianwei Jing, Jiafei Pang, Hang Lin, Zhenyu Qiu, and Changjun Liu*

Abstract—A multiband compact low-profile planar antenna based on multiple resonant stubs is proposed and studied. By utilizing two pairs of stubs embedded on a defected ground, the reflection coefficient less than -10 dB can be achieved with broadband characteristic for applications of wireless local area network (WLAN) and worldwide interoperability for microwave access (WiMAX). Meanwhile, a pair of inserted slots on both sides of a curve slot is applied to the antenna design, which decreases the cross polarization. A multiband antenna is fabricated and measured to verify the design. The antenna is compact with operation frequencies for WLAN (2.45/5.2/5.8 GHz) and WiMAX (2.8/3.8/5.5 GHz) applications. The measured peak gains are 5.5, 4.4, 0.0, and 5.6 dBi at 2.45, 2.8, 3.8, and 5.5 GHz, respectively.

1. INTRODUCTION

With the wide and rapid development of modern wireless communication, antennas with multiband operation are greatly demanded in mobile wireless communication terminals. Recently, to satisfy the applications of WLAN standards (2.45/5.2/5.8 GHz) and WiMAX standards (2.8/3.8/5.5 GHz), various types of planar multiband antennas have been investigated due to their compactness, low-profile, low-cost, and convenient fabrication, such as parasitic antennas, fractal antennas, and slot antennas [1–17].

In [1–3], multiband planar antennas with parasitic elements are proposed for WLAN and WiMAX wireless communications, which utilize various shaped stubs loaded around their radiation patch to achieve multiband characteristic. Another method to design multiband antennas is to use fractal geometry [4–7]. A low-cost fractal antenna loaded with parasitic edge coupled split ring resonators [4], a compact triple-band antenna for 2G, 3G, 4G, and sub-6 GHz 5G applications [5], and a Minkowski fractal-shaped loop antenna with a dielectric resonator [6] are presented, which have multiband performances and compact sizes. In [8–17], planar antennas adopt slot structures to operate at multiband frequencies. A monopole antenna with two identical split ring resonators employed on a defected ground to obtain 2.7, 4.3, and 4.7 GHz, respectively, is proposed in [8] with a dimension of $60 \times 60 \times 1.56 \text{ mm}^3$. In [9], three parallel rectangular open slots are etched on a ground plate of this antenna with a dimension of $50 \times 31.4 \times 1 \text{ mm}^3$ to generate multiple bands at GPS, Wi-Fi, and WiMAX. A capacitively coupled CPW-fed penta-band slot dipole antenna with a size of $70 \times 40 \times 0.508 \text{ mm}^3$ is investigated [10], which operates at 1.7, 2.5, 2.7, 3.1, and 3.7 GHz, and the peak gain is from 4 dBi to 5 dBi. However, collectively with these features, dimension, impedance matching bandwidth and cross polarization are still a challenge to limit the applications.

In this letter, a multiband monopole antenna with a dimension of $43 \times 33 \times 1.6 \text{ mm}^3$ operating at WLAN (2.45/5.2/5.8 GHz) and WiMAX (2.8/3.8/5.5 GHz) is proposed. Several stubs are embedded in its defected ground to resonate at various frequencies. A curved slot is etched on the ground below the microstrip feed line to enhance the bandwidth and improve the operating frequency. Meanwhile,

Received 11 July 2020, Accepted 11 September 2020, Scheduled 16 October 2020

* Corresponding author: Changjun Liu (cjliu@ieee.org).

The authors are with the School of Electronics and Information Engineering, Sichuan University, Chengdu 610064, China.

in order to cut down the cross polarization at high frequency, a pair of inserted slots is etched on both sides of the curve slot, which can reduce the cross range current distribution. The rest of this letter is organized as follows. The details of structure, comparison among four different ground plane structures, optimization of cross polarization, and current field distribution are discussed in Section 2. The experimental results are described in Section 3, where impedance matching bandwidth and field radiation patterns have a reasonable agreement with simulation. At the end, a conclusion about the superiority of this antenna is given in Section 4.

2. ANTENNA DESIGN

The geometry and configuration of the proposed antenna are shown in Figure 1. The dimension of this antenna is $43 \times 33 \times 1.6 \text{ mm}^3$. It consists of a microstrip feed line and a defected ground plane with multiple resonant stubs, which are printed on the top and bottom of an FR4 substrate ($\epsilon_r = 4.4$, $\tan \delta = 0.02$), respectively. A rectangular slot is etched on the ground plane to realize a low band. A ring slot corroded on the ground can add another current flow path to achieve an extra resonant frequency. The length of a affects impedance matching at the highest resonant frequency. Two pairs of unequal length rectangular stubs are connected to the rectangular ring slot ground plane to reach the other two different resonant frequencies. The length of each stub can be approximated from Equation (1), where c is the velocity of light in free space, f_0 the centre resonant frequency, and ϵ_r the dielectric constant of the substrate. Meanwhile, a pair of inserted slots is etched on sides of curve slot to decrease the cross polarization at upper band. This antenna is designed and simulated from ANSYS High Frequency

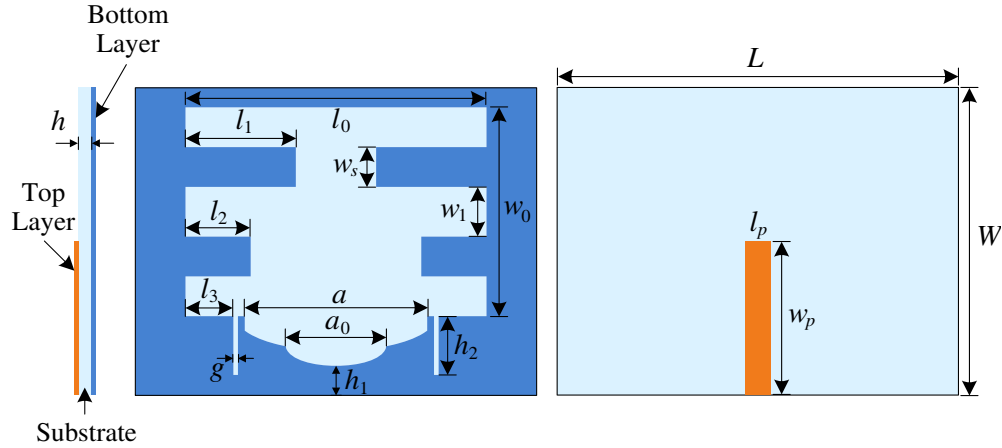


Figure 1. Geometry and configuration of the proposed antenna.

Table 1. Parameters of the proposed antenna.

Parameter	Value (mm)	Parameter	Value (mm)
L	43	W	33
l_p	2.75	w_p	17.5
l_0	33	w_0	23.1
l_1	12.1	w_1	5.5
l_2	7.15	w_s	4.4
l_3	5.25	h	1.6
a	20	h_1	3.3
a_0	11	h_2	6.5
g	0.5	–	–

Structure Simulator following the optimized parameters exhibited in Table 1.

$$L_{stub} = \frac{c}{4f_0 \sqrt{\frac{\epsilon_r + 1}{2}}} \tag{1}$$

The geometries of four antennas with various ground structures are shown in Figure 2, where simulated results of reflection coefficient ($|S_{11}|$) are illustrated. Antenna I is designed with a rectangular slot and a curve slot to obtain dual frequencies. Antenna II employs a pair of additional metal stubs to

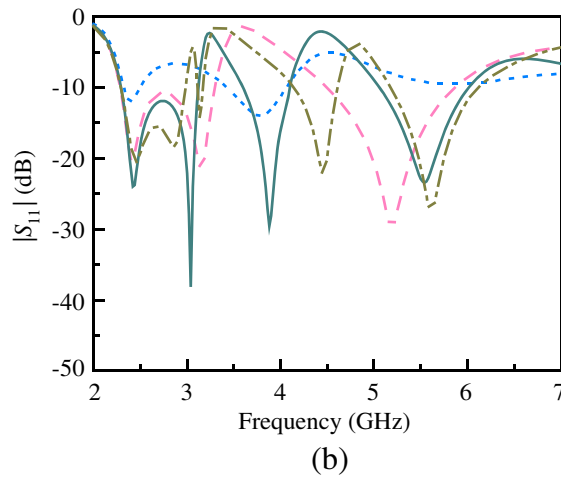
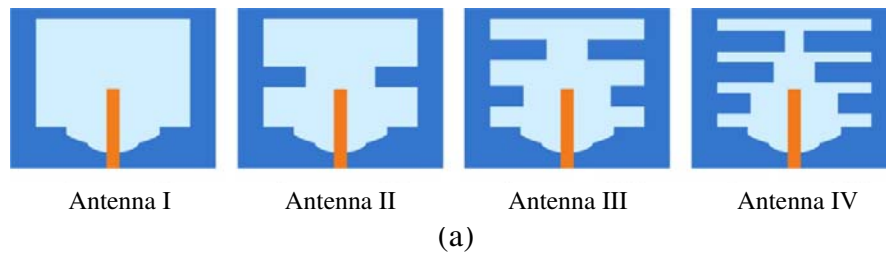


Figure 2. Performance comparison between antennas with various ground structures (a) configuration, (b) simulated result of $|S_{11}|$.

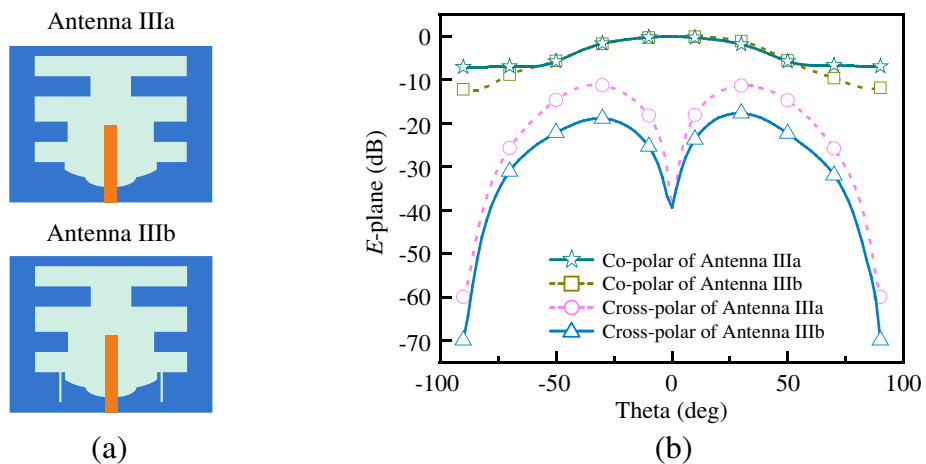


Figure 3. Comparison of cross polarization between the Antenna IIIa and Antenna IIIb, (a) structures of Antenna IIIa and Antenna IIIb, (b) simulated results.

resonate another frequency. Antenna III and Antenna IV utilize two and three pairs of stubs to obtain other two and three resonant frequencies, respectively. However, the bands of Antenna IV are narrow, and additional micro-strips will enhance the effect of cross polarization. Therefore, the optimal antenna is Antenna III by comparing with the four antennas. Furthermore, a pair of inserted slots can decrease cross range current and then improve antenna performance at high frequency. The comparison between an antenna without inserted slots (Antenna IIIa) and the proposed antenna (Antenna IIIb) is depicted in Figure 3. Note that the cross polarization decreases from -10 dB to -20 dB.

The simulated current field distribution of this antenna at resonant frequencies (2.45, 2.8, 3.8, and 5.5 GHz) is presented in Figure 4. It can be seen that the currents are located in different regions of the ground plane with increasing frequency. As illustrated in Figure 4(a) and Figure 4(d), the current flows mainly along the edge of the rectangular slot and loop slot to resonate in the lowest and highest frequencies. Meanwhile, as shown in Figure 4(b) and Figure 4(c), the current flows along the edge of the strips to resonate in the middle frequencies. Therefore, it justifies that the resonant frequencies are generated by etching slots on the ground plane.

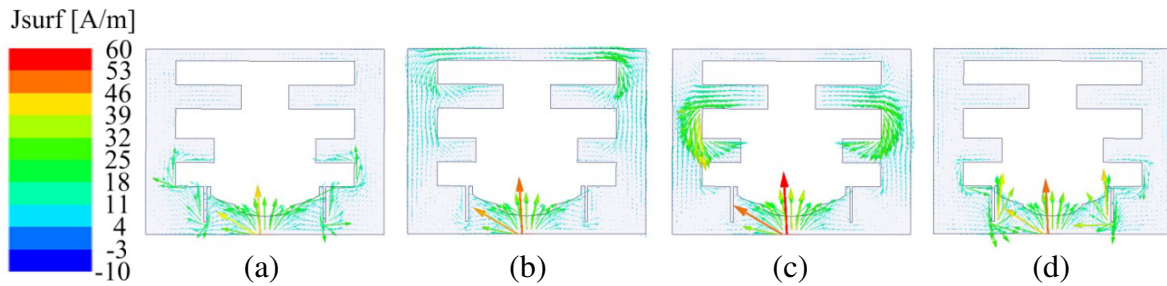


Figure 4. Distribution of current field, (a) 2.45 GHz, (b) 2.8 GHz, (c) 3.8 GHz, (d) 5.5 GHz.

3. MEASUREMENT RESULTS AND DISCUSSION

To further investigate the effectiveness of the proposed Antenna IIIb, the prototype of fabricated antenna is shown in Figure 5(a). A comparison between simulated and measured results of voltage reflection coefficient is illustrated in Figure 5(b). The measured result shows a great agreement with simulated

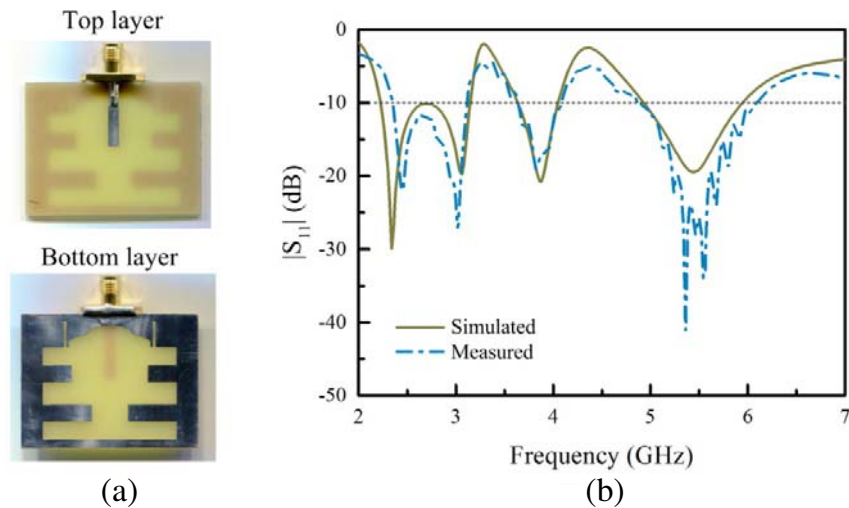


Figure 5. (a) Top layer and bottom layer of the prototype fabricated for the proposed antenna, (b) simulated and measured $|S_{11}|$.

one. The operating bands range from 2.28–3.10 GHz (30.4%), 3.52–4.10 GHz (15.2%), and 5.05–6 GHz (17.2%), which can be applied to WLAN and WiMAX with smaller than -10 reflection coefficient.

The simulated and measured far-field radiation patterns of this antenna at 2.45 GHz, 2.8 GHz, 3.8 GHz, and 5.5 GHz in E -plane (yz -plane) and H -plane (xz -plane) are exhibited in Figure 6, respectively. Note that there is a consistency between simulated and measured results. An

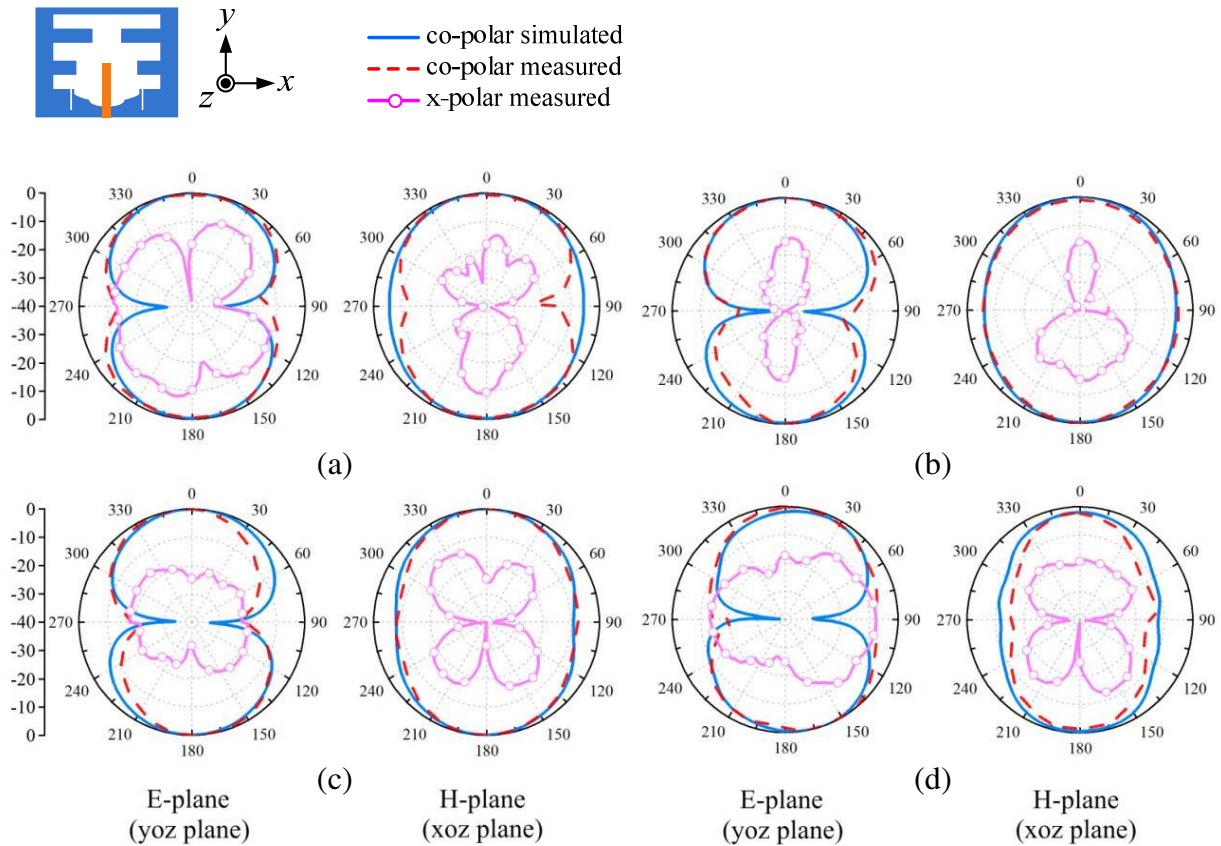


Figure 6. Measured and simulated normalized radiation patterns for proposed antenna at (a) 2.45 GHz, (b) 2.8 GHz, (c) 3.8 GHz and (d) 5.5 GHz.

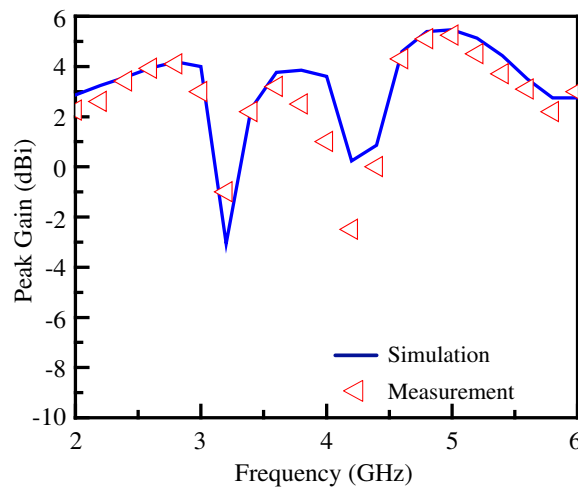


Figure 7. Measured peak gain of the proposed antenna.

omnidirectional radiation characteristic is displayed in H -plane, and a bi-direction radiation pattern is shown in E -plane with two opposite directions of $+z$ and $-z$. Again, the co-polarization of the fabricated antenna is 10 dB stronger than the x -polarization over the expected operating bands. Therefore, the proposed antenna has a stable radiation performance to receive or transmit electromagnetic wave. The measured peak gains of this antenna versus the operating frequencies are exhibited in Figure 7. It can be observed that the obtained peak gains are about 5.5, 4.4, 0.0, and 5.6 dBi for the 2.45-, 2.8-, 3.8-, and 5.5-GHz bands, respectively. These radiation characteristics reveal that the proposed antenna is competent for the WLAN and WiMAX applications.

4. CONCLUSION

With multiple resonant stubs utilized on the defected ground, a compact planar antenna is proposed and successfully fabricated for multiband applications in this letter. The measured reflection coefficients are greater than 10 dB in 2.28–3.10 GHz (30.4%), 3.52–4.10 GHz (15.2%), and 5.05–6.00 GHz (17.2%). In addition, the measured results show that the proposed antenna has good radiation characteristics, and peak gains are 5.5, 4.4, 0.0, and 5.6 dBi at 2.45, 2.8, 3.8, and 5.5 GHz, respectively. Meanwhile, the proposed antenna can be used to build an array with high bandwidth performance. In [18], a new approach to solve the problem of optimal power synthesis of array antennas is proposed, so that maximum possible bandwidth can be granted to fixed sidelobe-level performances. Therefore, this antenna also has a good high bandwidth performance for WLAN (2.45/5.2/5.8 GHz) and WiMAX (2.8/3.8/5.5 GHz) wireless communications.

REFERENCES

1. Kim, J.-W., T.-H. Jung, H.-K. Ryu, J.-M. Woo, C.-S. Eun, and D.-K. Lee, "Compact multiband microstrip antenna using inverted-L- and T-shaped parasitic elements," *IEEE Antennas and Wireless Propagation Letters*, Vol. 12, 1299–1302, 2013.
2. Kumar, A., J. K. Deegwal, and M. M. Sharma, "Design of multi-polarised quad-band planar antenna with parasitic multistubs for multiband wireless communication," *IET Microwaves, Antennas & Propagation*, Vol. 12, No. 5, 718–726, 2018.
3. Wen, L.-H., S. Gao, Q. Luo, Q. Yang, W. Hu, Y. Yin, X. Ren, and J. Wu, "A compact wideband dual-polarized antenna with enhanced upper out-of-band suppression," *IEEE Transactions on Antennas and Propagation*, Vol. 67, No. 8, 5194–5202, 2019.
4. Sharma, V., N. Lakwar, N. Kumar, and T. Garg, "Multiband low-cost fractal antenna based on parasitic split ring resonators," *IET Microwaves, Antennas & Propagation*, Vol. 12, No. 6, 913–919, 2018.
5. Alieldin, A., Y. Huang, S. J. Boyes, M. Stanley, S. D. Joseph, Q. Hua, and D. Lei, "A triple-band dual-polarized indoor base station antenna for 2G, 3G, 4G and sub-6 GHz 5G applications," *IEEE Access*, Vol. 6, 49209–49216, 2018.
6. Dhar, S., K. Patra, R. Ghatak, B. Gupta, and D. R. Poddar, "A dielectric resonator-loaded Minkowski fractal-shaped slot loop heptaband antenna," *IEEE Transactions on Antennas and Propagation*, Vol. 63, No. 4, 1521–1529, 2015.
7. Guo, L., W. Q. Chen, and W. C. Yang, "A novel miniaturized planar ultra-wideband antenna," *IEEE Access*, Vol. 9, 2769–2773, 2019.
8. Paul, P. M., K. Kandasamy, and M. Sharawi, "SRR loaded slot antenna for multiband applications," *2017 IEEE International Symposium on Antennas and Propagation & USNC/URSI National Radio Science Meeting*, 2017.
9. Li, W.-M., B. Liu, and H.-Y. Zhao, "Parallel rectangular open slots structure in multiband printed antenna design," *IEEE Antennas and Wireless Propagation Letters*, Vol. 14, 1161–1164, 2015.
10. Wu, Y. H. and W. H. Tu, "Compact Penta-band CPW-fed slot antenna," *IEEE 2018 International Symposium on Antennas and Propagation*, 1–2, 2018.

11. Dkiouak, A., A. Zakriti, and M. El Ouahabi, "Design of a compact dual-band MIMO antenna with high isolation for WLAN and X-band satellite by using orthogonal polarization," *Journal of Electromagnetic Waves and Applications*, Vol. 34, No. 9, 1254–1267, 2019.
12. Palandi, N. K., N. Nozhat, and R. Basiri, "Design and fabrication of small and low profile microstrip monopole antenna using CRLH-TL structures," *Journal of Electromagnetic Waves and Applications*, Vol. 33, No. 13, 1–15, 2019.
13. Pan, C. Y. and C. C. Su, "CPW-fed modified rhombus slot antenna with circularly polarized radiation for UHF RFID fixed reader application," *Journal of Electromagnetic Waves and Applications*, Vol. 30, No. 4, 559–569, 2020.
14. Qin, X. and Y. Li, "Compact dual-polarized cross-slot antenna with colocated feeding," *IEEE Transactions on Antennas and Propagation*, Vol. 67, No. 11, 7139–7143, 2019.
15. Singh, G., B. K. Kanaujia, V. K. Pandey, D. Gandwar, and S. Kumar, "Design of compact dual-band patch antenna loaded with D-shaped complementary split ring resonator," *Journal of Electromagnetic Waves and Applications*, Vol. 33, No. 16, 2096–2111, 2019.
16. Qi, L., S. Gao, Z. Chong, Z. Dawei, T. Chaloun, W. Menzel, V. Ziegler, and M. Sobhy, "Design and analysis of a reflectarray using slot antenna elements for Ka-band SatCom," *IEEE Transactions on Antennas and Propagation*, Vol. 63, No. 4, 1365–1374, 2015.
17. Yu, C., S. Yang, Y. Chen, and D. Zeng, "Radiation enhancement for a triband microstrip antenna using an AMC reflector characterized with three zero-phases in reflection coefficient," *Journal of Electromagnetic Waves and Applications*, Vol. 33, No. 14, 1846–1859, 2019.
18. Bui, L. T. P., N. Anselmi, T. Isernia, P. Rocca, and A. F. Morabito, "On bandwidth maximization of fixed-geometry arrays through convex programming," *Journal of Electromagnetic Waves and Applications*, Vol. 34, No. 5, 581–600, 2020.